

INVESTIGATIONS ON ANCIENT MORTARS FROM THE BASILIAN MONASTERY OF FRAGALÀ

Paola Cardiano^{1*}, S. Sergi¹, Concetta De Stefano¹, S. Ioppolo² and P. Piraino¹

¹Dipartimento di Chimica Inorganica, Chimica Analitica e Chimica Fisica, University of Messina, Salita Sperone 31 S. Agata 98166 Messina, Italy

²Dipartimento di Scienze Geologiche, Sezione di Mineralogia, Petrografia, Vulcanologia e Geochimica, University of Catania Corso Italia 55, 95129 Catania, Italy

The ancient mortars of the monastery of San Filippo di Fragalà in Frazzanò, the first Basilian-Norman center in Sicily, have been studied and classified by means of ICP, HPLC, TG-DTA, XRD and thin sections analysis. A new very simple method to evaluate the hydraulic properties of the mortars, based on the combination of analytical and thermogravimetric data, is also reported. The HPLC investigations indicate that the monastery is only partially involved in decay phenomena due to the action of soluble salts.

Keywords: hydraulic properties, mortars analysis, plasters analysis, soluble salts, thermal analysis, X-ray diffraction

Introduction

In a previous paper [1] we reported on the physico-chemical and mineralogical characterization of the ancient bricks of the monastery of San Filippo di Fragalà in Frazzanò, which represents the first Basilian–Norman center in Sicily and a national monument too (Fig. 1). Symbol of fifteen centuries of cultural life, the history of the monastery spans over 12 centuries beginning with the construction of the Byzantine church, followed by extension works of the original structure during the Norman period and concluding with the baroque and modern maintenance attempts. Today the monument suffers from extensive cracks, lost of joint mortars and finishing layer. Aim of the work is to gain further knowledge on the building history of the monastery through the physico-chemical and mineralogical characterization of bricks and mortars which are the main structural materials. The deep knowledge of the original materials has an impor-



Fig. 1 The monastery of ‘San Filippo di Fragalà’

tant bearing on the restoration and/or maintenance activity since only the selection and reproduction of materials physically and chemically compatible with the old ones allow the appropriate restoration activity to be developed [2]. As a notable example, the replacement of a joint lime mortar with a cementitious one, which is featured by different mechanical and microstructural properties, causes damage at the mortar/stone boundary region. The employment of cementitious mortar and concrete to restore the temple of Qasr al-Bint, Petra (Jordan) has led to severe damage of the structure as well as to the loss of the aesthetic value and authenticity of the monument [3].

Following our previous work we report here on the characterization and overall conservation state of the joint and finishing mortars of the monastery by a combination of ICP, XRD, TG-DTA and HPLC techniques. A new very simple method to evaluate the hydraulic properties of the mortars, based on the combination of analytical and thermogravimetric data, is also reported.

Experimental

The samples were taken according to historical and architectural considerations with the aid of archaeologists of ‘Soprintendenza ai Beni Culturali e Ambientali’ of Messina and are representative of three construction periods: Byzantine, Norman and Baroque. Notwithstanding the limitations imposed by the archeologists, in a few cases, sampling was per-

* Author for correspondence: pcardiano@unime.it

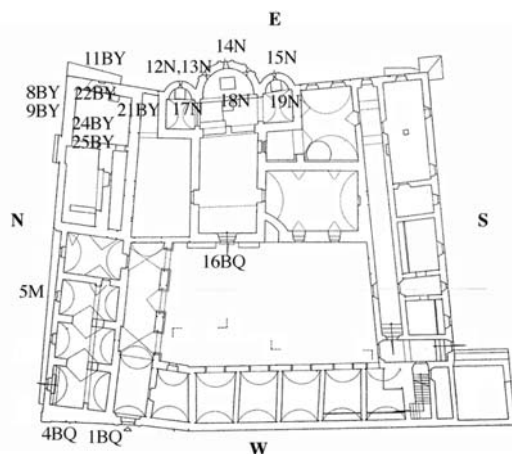


Fig. 2 Plan of the monastery and sampling points. Byzantine, Norman, Baroque, Modern

formed at different heights in order to study effects due to capillary rise. Sampling details about locations as well as age information are provided in Fig. 2. The mortars have been sampled with a chisel excluding their external portion in order to obtain materials not directly exposed to atmospheric pollutants. Thin polished sections of the samples were examined under an optical polarizing microscope (Zeiss). XRD investigations were carried out on Siemens D5000 diffractometer equipped with vertical goniometer, performing scans of 0.016°s^{-1} by means of CuK_α radiation ($\lambda=1.5406 \text{ \AA}$), with experimental conditions of 40 kV, 30 mA, 1 mm aperture diaphragm, 2 mm detector diaphragm and 1 mm scattered radiation diaphragm. Thin section as well as diffractometric analyses were performed both on the finest grains ($<63 \mu\text{m}$) and on the other fraction ($>63 \mu\text{m}$) obtained by sieving the samples through ISO565 series of sieves, thus allowing to detect binder/aggregate ratio as well. Major elements analyses were accomplished by inductively coupled plasma atomic emission spectrometry (ICP) by Activation Laboratories Ltd., Ancaster, Ontario, Canada. Water-soluble ions determination has been obtained following Normal recommendations [4] by extraction from finely grounded samples with a fixed volume of ultrapure water. The quantitative determination has been carried out with a Dionex Chromatographer equipped with the ED40 conductometric detector and isocratic pump. Data acquisition and elaboration were performed with the software package PeakNet 5.1. Thermogravimetric investigations have been carried out by means of PerkinElmer Pyris Diamond TG-DTA in the range $25\text{--}1000^\circ\text{C}$, under dynamic air (50 mL min^{-1}), with a heating rate of $10^\circ\text{C min}^{-1}$. Exact signal positions, including T_{max} and T_{onset} , were determined using a fitting software package (PeakFit 4, AISN soft. Inc.) assuming a convoluted Gaussian peaks profile. Microstructural charac-

teristics as well as mechanical properties were not investigated owing to crumbling samples.

Results and discussion

Mortars

Mortar is a composite material employed to assemble bricks or stones or as a finishing layer and it is obtained by the proper mixing of a binder with an inert fraction (also called aggregate). The function of the last is to improve the mechanical properties of the resulting material and to reduce, as much as possible, the shrinkage occurring during the hardening. It is mainly made of sand, clay, crushed stones, fossil fragments and it is mixed with the binder in different ratios. The binder, usually lime, hydraulic lime or, more rarely, dolomitic lime, is responsible for the hardening process. The mortar may also contain additives such as organic matter, gypsum, to improve workability and plasticity, and 'pozzolanic' materials, such as volcanic rocks, able to confer hydraulic properties to the final product. Literature reports [5–7] allow to group ancient mortars in two main categories: lime and hydraulic ones. In the first case the hardening process arises from carbonation of dry or wet lime [8]; on the contrary, if lime is associated also to argillaceous or pozzolanic materials, the reaction between these two phases leads to the formation of low-soluble calcium silicate hydrates or calcium aluminate hydrates which are responsible for the hydraulic behavior of the mortar. The resulting material, able to harden in presence of water, exhibit low porosity and enhanced mechanical properties with respect to pure lime mortars [9]. Among all the mortars, 'cocciopesto', used both as joint mortar or as a plaster [10], occupies a particular position. It was often employed as proof covering and as façade finishing layer and mainly contains lime, crushed bricks and other ceramic materials [11]. It is composed of fine-grained materials in order to obtain a smooth appearance when used as plaster. Owing to the presence of bricks the 'cocciopesto' mortars, widely used in the Roman and Byzantine periods, are reddish (due to iron oxides) and may exhibit hydraulic character too. The reaction, at the brick/lime boundary region, between lime and the bricks silicates leads in fact to the formation of calcium silico-aluminate hydrates.

Although in principle historical mortars may be differentiated on the basis of the binder/aggregate ratio and on the nature of both the components, their exact reproduction shows several drawbacks due to: a) chemical transformations and degradation phenomena occurring during hardening as well as over the times that lead to the formation of new species; b) the

binder/aggregate ratio that cannot be accurately estimated. Binder and inert fragments ought to be featured by different granulometry, being the binder grains finer. The widely accepted method to separate the two components involves the sieving of the bulk sample through the ISO565 series with meshes of 0.063 mm. The fraction with particle size $<63 \mu\text{m}$ is the most significant being mainly composed of binder while the fraction with granules $>63 \mu\text{m}$ ought to include all the aggregate. The not uncommon presence of low-grained inert ($<63 \mu\text{m}$) fragments leads to overestimate the binder/aggregate ratio while binding material, strongly stuck to aggregate granules, leads to underestimate the above ratio. Furthermore, attempts to exactly evaluate the amount of aggregate through the attack by more or less concentrated HCl [12] are vanished when in this fraction calcareous stones or other soluble components are present.

ICP analysis

Based on the MgO content the mortars may be grouped in two sets: set I featured by an MgO content lower than 2% (Table 1) and set II, namely 12N, 13N, 14N, 15N and 18N, all belonging to the Norman age, with an MgO content lying in the range 6.12–11.39%. Among the samples of set II, sample 13N displays the highest MgO content and it is also featured by a thermogravimetric behavior quite different with respect to that of 12N, 14N, 15N, taken in the external apses, and 18N sampled inside the central apse of the Norman church. It is not clear whether the high MgO content of these samples comes from a pure coincidence or whether it was a matter of choice of the original masons. It is worth to note that mortars also containing magnesian lime are featured by improved resistance to water associated to lower viscosity with respect to pure lime mortars.

The low MgO content samples comprise the remaining Norman samples, as well as the Baroque and the Byzantine ones. Differently from the other Norman mortars, 17N and 19N, sampled in the internal apses of the Norman church, contain very low amount of MgO but, at the same time, they differ considerably for the SiO_2/CaO (0.89 for 17N and 2.60 for 19N) and $\text{CaO}/\text{Fe}_2\text{O}_3$ (24.20 for 17N and 8.50 for 19N) ratios evidencing a higher inert/binder ratio for 19N. This is also supported by thin-section analysis that evidences a higher amount of quartz and quartzite in sample 19N. In our opinion 17N and 19N are not so different as they appear. We suppose that the sensible difference in the above cited ratios is mainly due to sampling operations. It is worth to remember that archeologists did not allow us extensive sampling; so it is reasonable to suppose that we recovered for 19N

Table 1 Major oxides/%

Samples	SiO_2	Al_2O_3	Fe_2O_3	MgO	CaO
8BY	43.63	3.81	1.67	0.96	23.46
9BY	46.25	5.44	2.35	1.08	19.05
11BY	50.17	3.89	2.36	1.93	20.72
21BY	7.51	1.49	0.64	3.31	45.37
22BY	48.08	3.57	1.92	1.95	22.43
24BY	18.80	3.76	1.41	0.58	34.96
25BY	22.74	4.44	1.78	0.61	34.51
12N	33.66	2.97	1.25	6.12	26.70
13N	31.15	2.67	1.22	11.39	21.76
14N	38.42	3.27	1.70	8.24	21.11
15N	26.82	2.84	1.37	7.25	28.43
17N	30.11	3.23	1.39	0.84	33.64
18N	29.68	2.78	1.11	9.78	23.01
19N	51.14	5.33	2.31	1.00	19.64
1BQ	34.54	11.68	4.28	1.01	24.06
4BQ	33.20	10.78	4.27	0.95	25.30
16BQ	32.69	9.44	3.66	1.00	26.41
5M	43.74	6.97	3.79	0.80	20.52

a fraction richer in aggregate. Based on analytical data only, we may anticipate that the Norman samples may be subgrouped since the outer and the inner part of central apses were made by employing a dolomitic lime while pure lime was used for the inner part of left and right apses.

The finishing mortars 1BQ and 4BQ, taken from the monastery main portal, and 16BQ, sampled on the portal of the church, appear quite similar and are representative of the only plasters still surviving in the monastery. They show the highest Fe_2O_3 content (3.66–4.28%) according to the presence in the aggregate fraction of crushed bricks that confer a red color to the samples and that allow to classify them as ‘cocciopesto’ mortars. They exhibit also comparable SiO_2/CaO , $\text{SiO}_2/\text{Al}_2\text{O}_3$ and $\text{SiO}_2/\text{Fe}_2\text{O}_3$ ratios suggesting that either the main façade as well as the portal were restored in the same period. The joint mortar 5M, dated back to 1930, displays a composition compatible with a crushed-brick mortar, with a Fe_2O_3 content comparable to the Baroque cocciopesto samples.

Based on the data gathered in Table 1 the Byzantine samples 8BY, 9BY, 11BY and 22BY, taken from the outer and inner side of the Byzantine church respectively, may be grouped separately from the light-red colored 24BY and 25BY as they are featured by highest inert/binder ratios, as evidenced by the SiO_2/CaO , $\text{Al}_2\text{O}_3/\text{CaO}$ and $\text{Fe}_2\text{O}_3/\text{CaO}$ ratios, considerably higher than those displayed by 24BY and 25BY. Furthermore, beside to be featured by a high amount of binder fraction, 24BY and 25BY exhibit an aggregate also com-

posed of small pieces of crushed bricks. The sample 21BY cannot be included in set II, since it is featured by an MgO content of 3.31%, nor in set I being mainly made of binder ($\text{SiO}_2/\text{CaO}=0.16$).

X-ray analysis

The macroscopic examination of the samples provides evidence of a great variety in terms of color and consistency while thin section observations, carried out by means of a polarizing microscope (beside the texture, the microscopic analysis allows to detect minerals featured by the same chemical composition but different crystalline habit), showed that the whole of the samples are featured by a fine-grained carbonatic matrix, with a color varying from gray to gray-brown and red-brown. Quartzite and quartz have been detected in the aggregate fraction of all the samples while calcite dominates the binder fraction. The pores featuring the majority of the samples are mainly small, spherical or egg-shaped, rarely elongated, with heterogranular clasts, different in terms of size and composition.

The crystalline phases present in the samples were detected by XRD investigations on finely pulverized mortars [13]. The XRD patterns clearly indicate that calcite, quartz and, to a lesser extent, micas (biotite and muscovite) can be recognized as common phases pres-

ent in all the samples (Table 2) while the other minerals are present in small quantities or in traces.

The Norman samples 12N, 13N, 14N, 15N, 18N appear quite similar being the binder mainly composed of primary calcite and the aggregate of quartz and quartzite. In addition to dolomite $\text{CaMg}(\text{CO}_3)_2$, they also contain fillosilicates, such as chlorite $(\text{Fe,Mg,Al})_6(\text{Si,Al})_4\text{O}_{10}(\text{OH})_8$, biotite $(\text{K,Fe,Mg})_3\text{AlSi}_3\text{O}_{10}(\text{F,OH})_2$, and muscovite $(\text{KAl}_2(\text{AlSi}_3\text{O}_{10})(\text{F,OH})_2)$, and plagioclase $(\text{CaAl}_2\text{Si}_2\text{O}_8-\text{NaAlSi}_3\text{O}_8)$. Small quantities of hydraulic minerals, such as boggsite $(\text{NaCa}_2(\text{Al}_5\text{Si}_{19}\text{O}_{48})\cdot 17\text{H}_2\text{O})$, dellaite $(\text{Ca}_6\text{Si}_3\text{O}_{11}(\text{OH})_2)$, found also in samples 1BQ, 9BY and 21BY, and wairakite $(\text{CaAl}_2\text{Si}_4\text{O}_{12}\cdot 2\text{H}_2\text{O})$ characterize the samples 12N, 13N, 14N, 15N and 18N while 17N and 19N, as suggested on the basis of ICP analysis, show different mineral distribution. In addition sample 19N shows well detectable traces of gypsum $(\text{CaSO}_4\cdot 2\text{H}_2\text{O})$ and ettringite $(\text{Ca}_6\text{Al}_2(\text{SO}_4)_3(\text{OH})_{12}\cdot 26\text{H}_2\text{O})$. Although the latter is usually associated to gypsum degradation processes [14], i.e. the reaction of calcium alumino-silicate hydrate or calcium carbonate with sulphur compounds from atmospheric origin, we believe that the presence of gypsum, also detected in 21BY, and its degradation products in sample 19N and 21BY may be ascribed to the raw materials rather than to a degradation process. Montmorillonite, $(\text{AlMg})\text{Si}_4\text{O}_{10}(\text{OH})_2\text{Na}$ (its pres-

Table 2 XRD data (Qz, quartz; Cc, calcite; Do, dolomite; Pl, plagioclase; Kf, K-feldspar; De, dellaite; Go, goethite; Bt, biotite; Ms, muscovite; Ch, chlorite; Mn, montmorillonite; Et, ettringite; Ta, taumasite; Ep, epidote; An, amphibole; Bg, boggsite; Wa, wairakite; Gy, gypsum)

Samples	Qz	Cc	Do	Pl	Kf	De	Go	Bt/Ms	Ch	Other minerals
8BY	xxx	xxx			x			x	x	An
9BY	xxx	xxx				x		x	x	Bt
11BY	xxx	xxx	x	x				x	x	
21BY	xx	xxx	x		x			x	x	Gy
22BY	xxx	xxx	x	x	x			x	x	
24BY	xxx	xxx		x	x		x	x	x Mn	
25BY	xxx	xxx					x		x Mn	
12N	xxx	xxx	x	x		x		x		Bg Wa
13N	xxx	xxx	x	x	x	x		x	x	Bg Wa
14N	xxx	xxx	x	x		x				Bg Wa
15N	xxx	xxx	x			x			x	Bg Wa
17N	xxx	xxx			x				x	
18N	xxx	xxx	x	x		x		x	x	Bg Wa
19N	xxx	xxx						x	x	Et Gy
1BQ	xxx	xxx		x	x	x	x		Mn	
4BQ	xxx	xxx			x		x	x	Mn	Et and/orTa
16BQ	xxx	xxx	x		x		x		Mn	
5M	xxx	xxx		x				x		Ep

ence may be associated to the crushed bricks of the inert), goethite $\text{FeO}(\text{OH})$, due to the oxidation of iron in hydrated environment and K-feldspar (KAlSi_3O_8) have been detected in Baroque *cocciopesto* mortars and, to a lesser extent, in samples 24BY and 25BY only. Investigations on the thin sections of the above '*cocciopesto*' samples by polarizing microscope reveal the presence of crushed bricks together with fragments of metamorphic rocks, quartz, and, in some cases, primary and secondary calcite (according to what before stated, primary and secondary calcite can be detected by thin section analysis only). In Fig. 3 the thin section of a typical *cocciopesto* structure, referred as 'reaction rim', can be observed. It arises from the well known 'pozzolanic' reaction between lime and silica and/or quartz leading to the formation of calcium silicate and aluminate hydrate. The reaction occurs at the binder/aggregate interface, lowering discontinuities between the two phases and improving the mechanical properties of the resulting materials.

The XRD pattern of the Byzantine samples, despite the differences evidenced by ICP analysis, appear comparable. Chlorite, biotite, K-feldspar and plagioclase, in small quantities or just in traces, are mineral phases common to all the samples. In the thin section analysis of sample 21BY, mainly made of binder, two binder fractions can be distinguished: the first compact and fine-grained with few micropores, tiny fragments of quartz crystals as well as sedimentary material, the other fine-grained but with more abundant small quartz clasts and a medium amount of pores. The XRD analysis on this sample also shows the presence of gypsum, K-feldspar, micas and chlorite.

Thermogravimetric and differential thermal analysis

Differential thermal and thermogravimetric analyses are very useful tools for the characterization of ancient mortars. They allow detecting mortars' main components, such as calcite, lime, magnesite (MgCO_3), gypsum, organic additives, phenomena associated to clay degradation as well as dehydration of hydraulic minerals. As previously stated, the binder of a mortar may be aerial, that implies a mortar made by mixing the aggregate with lime only, and hydraulic, that means addition to lime of hydraulic materials such as pozzolana, ashes or argillaceous materials that over the time react with lime giving hydraulic minerals. The substitution of pure lime mortar with hydraulic one, featured by lower porosity and better mechanical properties, may cause severe damages at the boundary region between new and original material. Until now, the determination of mortar hydraulicity has been mainly based on thermogravimetric

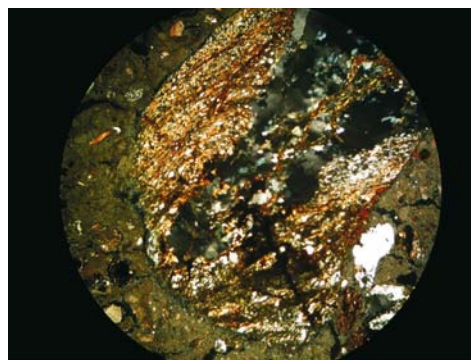


Fig. 3 Thin section for a *cocciopesto* sample showing the 'reaction rim' between crushed brick and the binder. Crossed nicols, 50 \times

investigations by evaluating the ratio between the CO_2 (arising from decomposition of calcitic materials) and the amount of chemically bound water, that is related to the presence of hydraulic materials (water loss from calcium silicate hydrates and calcium aluminate hydrates) [9]. Low values of the $\text{CO}_2/\text{H}_2\text{O}$ ratio, associated to values of CO_2 below 30%, are indicative of the presence of hydraulic compounds. In our opinion this method suffers from some drawbacks. The chemically bound water is evaluated through the mass loss of the binder fraction in the temperature range 200–600°C. But if argillaceous materials, that in the same temperature range undergo interlayer water loss and dehydroxylation, are present, then the total mass loss in the above range cannot be accounted for the evaluation of hydraulic mineral phases only. So this method, that perhaps considers a very large temperature range, is reliable only if the binder does not contain fillosilicates such as montmorillonite, muscovite, chlorite and illite. Furthermore the CaO content recovered from chemical analysis ought to be appreciably higher than the CaO content, as indirectly detected by thermogravimetric analysis, indicating that calcium containing minerals other than carbonates are present. In this paper the evaluation of the hydraulicity was performed through the combination of analytical and thermogravimetric data. When the amount of CaO (CaO_{TGA}), as found by thermogravimetric analysis and calcimetry (Fruhling method), corresponds to the CaO content, as determined by ICP analysis (CaO_{ICP}), the mortar is definitely aerial. When the ratio $\text{CaO}_{\text{ICP}}/\text{CaO}_{\text{TGA}}$ is higher than 1, the exceeding CaO content may be related to Ca containing hydraulic minerals. Furthermore, this method does not require the problematic separation binder/inert.

The TG patterns in dynamic air of the Baroque *cocciopesto* mortars (1BQ, 4BQ and 16BQ), (binder/aggregate ratio 1:2.2–2.8) show the following common features: *i*) a main mass loss at $\sim 715^\circ\text{C}$, due to calcite decomposition; *ii*) two minor endothermic peaks, the

first below 100°C (~1%), assigned to the loss of hygroscopic water, and the second, in the range 350–600°C (Table 3), due to phenomena associated to clay degradation (interlayer water loss and clay dehydroxylation) and to dehydration of hydraulic components of the bricks fragments. An additional peak, exothermic in nature, is detected at ~300°C very likely due to combustion of small amounts of organic materials added to improve plasticity [15]. The Byzantine mortars 24BY and 25BY (binder/aggregate ratio ~1:1.6–1.8), featured by the presence of crushed bricks as well, differ from the Baroque *cocciopesto* ones due to the higher mass loss in the calcite decomposition range, according to ICP data that evidence for the former higher CaO/SiO₂ ratios. At the same time mortar 5M, dated back to 1930, displays thermal properties quite similar to the Baroque ones. In order to compare the thermal behavior of all the aforementioned mortars, the fitting and the deconvolution of the DTG curves have been performed. The analysis of the deconvoluted curves showed that the *cocciopesto* mortars, as well as 24BY and 25BY, are characterized by the same processes although different in intensities. In addition, as already stated, the Baroque mortars display a signal with T_{\max} at 300°C due to the combustion of organic matter.

The TG curves of the Norman samples 12N, 14N and 15N and 18N (binder/aggregate ratio ~1:2.5) are very similar except for a higher organic material content for sample 15N. They show a main inflection, due to calcite decomposition, at about 670°C, associ-

ated with a continuous mass loss starting from 420 to 550°C, ascribed to clay degradation and dehydration of aluminosilicate. The thermogravimetric investigations do not allow to clarify the nature of the Mg containing minerals of which the above samples are richer. Usually the only Mg containing minerals detectable by thermogravimetric analysis are brucite Mg(OH)₂ (mass loss in the range 350–420°C), hydromagnesite 4MgCO₃·Mg(OH)₂·4H₂O (mass losses at 250, 385 and 440–520°C), dolomite (two inflections at 780 and 860°C) and magnesite (mass loss in the range 550–620°C). Unfortunately the signals associated to these species lie in the same temperature range were calcite decomposition, clay degradation and calcium aluminosilicates dehydration occur. The only significant information was obtained by recording the thermogravimetric curves of the aggregate fraction of the above samples. They show the main inflection at 610°C, easily assigned to magnesite decomposition. As a consequence the broad inflection, detected in the TG curves of the bulk samples in the range 600–800°C, includes either the calcite as the magnesite decomposition. The other two samples 17N and 19N (binder/aggregate ratio ~1:1.8), taken in the inner part of left and right apse, respectively, are without doubt, as previously anticipated, different from samples 12N, 14N and 15N sampled in the external part of the three apses and even different from 18N, taken in the inner part of the central apse. They also differ between them for the mass loss in the range 600–800°C, very likely due to a higher amount of inert in 19N. Sample 13N (binder/aggregate ratio ~1:3) appears very different from the others as it shows a main inflection at 698°C, easily assigned to calcareous material decomposition. It is worth to remember that for calcite decomposition a temperature range rather than a specific temperature may be defined. The decomposition of calcitic materials in fact may vary in a large temperature range (650–850°C) as a function of the history of the material (it may contain recarbonated lime), experimental conditions, degree of fragmentation and crystallinity of the material. Monocrystalline calcite undergoes complete decarbonation at temperatures higher than 750°C while polycrystalline materials, such as limestone or chalk, in some cases start to decompose at temperatures lower than 650°C [5, 16]. The TG curve of 13N also shows a sharp peak, endothermic in nature, at 108°C, probably due to dehydration of small amount of gypsum, absent in the XRD patterns, and an envelop of signals culminating at 468 and 502°C. Since this mortar was sampled on the basis of the single lancet window, it could be the result of restoration activity.

Similar inflections appear to feature the TG curves of the Byzantine mortars 8BY, 9BY (binder/

Table 3 Thermogravimetric data/mass loss%

	<200°C	200–350°C	350–600°C	>600°C	Res./%
8BY	1.8	2.8	4.6	16.9	73.9
9BY	1.9	3.0	4.4	15.6	74.8
11BY	0.6	0.7	1.3	15.9	81.5
21BY	1.1	0.9	1.4	34.0	62.6
22BY	0.6	0.5	1.2	17.5	80.2
24BY	1.3	2.0	2.2	26.9	67.6
25BY	1.2	1.5	2.1	24.0	71.1
12N	1.4	1.7	3.1	22.2	71.2
13N	2.0	0.8	6.4	13.0	77.8
14N	2.1	1.9	3.6	19.7	72.4
15N	1.6	3.6	2.8	21.3	70.8
17N	0.8	1.4	2.4	24.9	70.6
18N	0.7	0.9	4.4	24.2	69.8
19N	1.1	1.3	2.2	15.2	80.2
1BQ	1.2	1.5	1.5	17.2	78.6
4BQ	0.8	1.5	1.4	17.5	78.8
16BQ	1.3	1.7	1.9	18.5	76.6
5M	0.8	1.6	2.0	15.8	79.7

aggregate ratio ~1:3), 11BY and 22BY (binder/aggregate ratio ~1:2.5). Although the mass loss in the range 600–800°C is predominant in all the samples, 8BY and 9BY, taken in the same area but in the outer wall at different heights, exhibit, in the temperature range 350–600°C, a structurally water content three times higher than the one displayed by 11BY and 22BY that appear mainly made of calcitic materials with a higher amount of inert.

As far as the classification of mortars sampled in the monastery of Frazzanò is concerned (Table 4) we note that the majority appears mainly made of aerial binding with minor amounts of hydraulic compounds. This suggestion is based on the $\text{CaO}_{\text{ICP}}/\text{CaO}_{\text{TGA}}$ ratios (appropriately corrected for samples 12N, 13N, 14N, 15N and 18N which contain not negligible amounts of MgCO_3) that for most of the samples correspond to values slightly above 1. This means that almost all the CaO found by ICP arises from calcite and that the amount of calcium silicate or calcium aluminate is scarce. In Table 4 are also reported the values of the ratio $\text{CO}_2/\text{H}_2\text{O}$, calculated as suggested by literature reports [5, 9, 11, 17–19] and the ratio $\text{CaO}_{\text{ICP}}/\text{CaO}_{\text{TGA}}$. It can be noticed that samples, such as 8BY and 9BY, featured by low values of the $\text{CO}_2/\text{H}_2\text{O}$ ratios, indication of enhanced hydraulic character according to literature, exhibit $\text{CaO}_{\text{ICP}}/\text{CaO}_{\text{TGA}}$ values little higher than 1, suggesting that almost all the CaO content arises from calcitic materials with little amounts of

hydraulic compounds. Based on the combination of ICP and thermogravimetric analyses the Byzantine mortars appear mainly made of calcitic binder while for the Baroque cocciopesto mortars, featured by a $\text{CO}_2/\text{H}_2\text{O}$ ratio ranging from 5.1 to ~6, the hydraulic character is not enhanced being little more than 1 the $\text{CaO}_{\text{ICP}}/\text{CaO}_{\text{TGA}}$ ratio. The two methods lead to similar results for Norman samples 12N, 13N, 14N, 15N, 18N and for the Byzantine 21BY. Both the indicators in fact suggest to classify the Norman samples as hydraulic lime mortars and 21BY as a pure lime mortar. The hydraulic character is even more enhanced in sample 13N, featured by a $\text{CaO}_{\text{ICP}}/\text{CaO}_{\text{TGA}}$ ratio of 1.37 and hydraulicity index, evaluated on the basis of the $\text{CO}_2/\text{H}_2\text{O}$ ratio, very low (~1.8).

Soluble salts analysis

In order to assess the whole conservation state of the mortars, the determination of soluble salts content was carried out. It is well ascertained in fact that ‘salt decay’ represents the main deterioration cause involving ancient lithic materials such as stones, bricks and mortars. Soluble salts may originate from air pollution, marine spray, groundwater capillary rise; they may be present in the original raw materials as well. Supersaturation of salts solutions confined within the pores leads to formation of crystals which, on growing, exert stress on the pore walls. When the so-called ‘crystallization pressure’ exceeds the tensile strength of the lithic material, disruption occurs [20–22]. Usually high contents of alkali nitrates, chlorides and sulphates correspond to weakened structures.

As already found for the bricks belonging to the same building, soluble salts determination on the mortars of the monastery of San Filippo di Fragalà shows that the deterioration of the old building, although at first sight this could appear surprising, cannot be mainly ascribed to phenomena associated to salts crystallization. Only the samples 8BY and 9BY (Table 5), taken from the northern wall, show appreciable amounts of chloride, sulphate and nitrate ions while all the other samples, even those sampled in the external part of the eastern wall do not show considerable amounts of the above salts. These findings may be explained looking at the geographical location of the Monastery. The southern, eastern and western sides of the building are protected by mountains which do not allow to marine spray or other pollutants to reach the above zones. The northern side only, although quite far from the sea, is exposed to the atmospheric pollutants. Furthermore, the low salt content featuring almost all the samples indicates that the building, being built on the rocks, is not affected by rising dump phenomenon. Table 5 clearly shows that

Table 4 Comparison between the two methods of evaluating the mortars’ hydraulic properties

Samples	$\text{CO}_2/\text{H}_2\text{O}$	$\text{CaO}_{\text{ICP}}/\text{CaO}_{\text{TGA}}$
8BY	2.28	1.09
9BY	2.11	1.05
11BY	7.95	1.03
21BY	14.78	1.04
22BY	10.29	1.01
24BY	6.40	1.03
25BY	6.67	1.13
12N	4.62	1.19
13N	1.81	1.37
14N	3.58	1.20
15N	3.33	1.22
17N	6.55	1.07
18N	4.57	1.19
19N	4.34	1.01
1BQ	5.73	1.10
4BQ	6.03	1.14
16BQ	5.14	1.12
5M	4.39	1.03

Table 5 Soluble salts content/%

	Cl ⁻	NO ₂ ⁻	NO ₃ ⁻	SO ₄ ²⁻	PO ₄ ³⁻	Na ⁺	K ⁺	NH ₄ ⁺	Mg ²⁺	Ca ²⁺
8BY	0.80	–	1.28	0.73	–	0.56	0.44	0.02	0.07	1.17
9BY	0.89	–	1.57	0.61	0.11	0.29	0.37	0.04	0.08	0.98
11BY	0.08	0.01	0.07	0.30	–	0.43	0.09	0.01	0.03	0.74
21BY	0.03	–	0.09	0.17	0.14	0.45	0.10	–	0.05	0.56
22BY	0.11	–	0.19	0.03	0.06	0.39	0.09	0.01	0.03	0.59
24BY	0.03	–	0.12	0.19	0.04	0.28	0.15	0.01	0.02	0.59
25BY	0.03	–	0.09	0.12	–	0.23	0.12	0.01	0.02	0.80
12N	0.08	–	0.12	0.09	0.30	0.55	0.09	0.02	0.03	0.74
13N	0.30	–	0.23	0.33	0.20	0.48	0.08	0.01	0.05	0.74
14N	0.04	–	0.07	0.11	0.09	0.52	0.09	–	0.08	0.68
15N	0.04	–	0.07	0.14	0.22	0.54	0.06	–	0.27	0.62
17N	0.21	–	0.25	0.13	0.21	0.46	0.07	–	0.28	0.56
18N	0.67	–	0.91	0.19	0.11	0.57	0.12	0.01	0.07	0.58
19N	0.04	–	0.09	0.03	0.16	0.45	0.11	0.01	0.06	0.62
1BQ	0.15	0.01	0.05	0.05	–	0.47	0.13	0.03	0.02	0.65
4BQ	0.05	–	0.11	0.08	–	0.11	0.08	0.03	0.01	0.62
16BQ	0.04	–	0.06	0.04	0.33	0.43	0.04	–	0.48	0.61
5M	0.06	–	0.06	0.04	–	0.13	0.11	0.04	0.01	0.52

detectable amounts of sulphates have been found in samples 13N and 11BY too. Since no other relevant data have been detected for these samples their anionic content can be ascribed to the original composition of the raw materials rather than to a specific alteration.

Conclusions

Despite the limited number of the investigated samples does not permit a statistical treatment of the data, the outcome of all the analyses carried out on the ancient mortars sampled in the monastery of San Filippo di Fragalà allows some conclusions to be drawn. Based on the combination of analytical, XRD and thermogravimetric investigations, most of the mortar samples analyzed, except the Norman ones, were mainly made of calcite and aggregate with minor amounts of hydraulic minerals. The whole of the investigations also allows grouping the samples in six classes at least. One class comprises the cocciopesto mortars 1BQ, 4BQ and 16BQ, used as finishing layers. These samples give quite homogeneous responses to all the investigations. Sample 5M, a joint mortar containing crushed brick and falling into the ‘cocciopesto’ categories too, is dated to 1930 according to the inscription clearly readable on the northern wall.

Samples dated back to the Norman age must be subgrouped since they vary for chemical composition, thermogravimetric and mineralogical features. The first difference lies in the MgO content. Samples

12N, 13N, 14N, 15N and 18N are featured by a considerable amount of MgO, whose nature we were only partially able to discover, while 17N and 19N, with a MgO content of ~1%, must be grouped separately. The latter samples also differ between them for the binder/inert ratio but, based on mineralogical and thermogravimetric findings, we suggest that they belong to the same subgroup. Sample 13N, featured by the highest MgO content (13%), cannot be grouped with 12N, 14N, 15N and 18N since all the analyses suggest for 13N a different composition. It exhibits the highest CaO_{ICP}/CaO_{TGA} ratio (1.37) that allows to classify it as a hydraulic mortar. The Byzantine samples are not homogeneous as well. They may be confidently classified as follows: group A comprising 8BY, 9BY, 11BY and 22BY; group B including 24BY and 25BY, in which the aggregate clearly was made also using crushed bricks; and sample 21BY, mainly made of binder.

Furthermore, despite their age, the monastery mortars display a moderate salts content suggesting that ‘salt decay’ phenomenon is only partially responsible for its deterioration.

References

- 1 P. Cardiano, S. Ioppolo, C. De Stefano, A. Pettignano, S. Sergi and P. Piraino, *Anal. Chim. Acta*, 519 (2004) 103.
- 2 C. Tomasi, O. Ricci, G. Perotti and P. Ferloni, *J. Therm. Anal. Cal.*, 84 (2006) 33.

ANCIENT MORTARS FROM THE BASILIAN MONASTERY OF FRAGALÀ

- 3 Z. Al-Saad and M. A. H. Abdel-Halim, *Eng. Struct.*, 23 (2001) 926.
- 4 Normal Protocol 13/83, *Dosaggio dei sali solubili*, CNR-ICR, Rome, 1983.
- 5 A. Moropoulou, A. Bakolas and K. Bisbikou, *Thermochim. Acta*, 269/270 (1995) 779.
- 6 G. Chiari, M. L. Santarelli and G. Torraca, *Materiali e Strutture*, 3 (1992) 111.
- 7 M.P. Riccardi, P. Duminuco, C. Tomasi and P. Ferloni, *Thermochim. Acta*, 321 (1998) 207.
- 8 E. T. Stepkowska, M. A. Aviles, J. M. Blanes and J. L. Perez-Rodriguez, *J. Therm. Anal. Cal.*, 87 (2007) 189.
- 9 A. Moropoulou, A. Bakolas and K. Bisbikou, *J. Cultural Heritage*, 1 (2000) 45.
- 10 H. Boke, S. Akkurt, B. Ipekoglu and E. Ugurlu, *Cem. Concr. Res.*, 36 (2006) 1115.
- 11 A. Bakolas, G. Biscontin, A. Moropoulou and E. Zendri, *Thermochim. Acta*, 321 (1998) 151.
- 12 J. I. Alvarez, A. Martin, P. J. Garcia Casado, I. Navarro and A. Zornoza, *Cem. Concr. Res.*, 29 (1999) 1061.
- 13 B. Middendorf, J. J. Huges, K. Callebaut, G. Baronio and I. Papavianni, *Mater. Struct.*, 38 (2005) 761.
- 14 C. Sabbioni, G. Zappia, C. Riontino, M. T. Blanco-Varela, J. Aguilera, F. Puertas, K. Van Balen and E. E. Toumbakari, *Atmos. Environ.*, 35 (2001) 539.
- 15 P. Bruno, D. Calabrese, M. Di Pierro, A. Genga, C. Laganara, D. A. P. Manigrassi, A. Traini and P. Ubbriaco, *Thermochim. Acta*, 418 (2004) 131.
- 16 S. Shoval, M. Gaft, P. Beck and Y. Kirsh, *J. Thermal Anal.*, 40 (1993) 263.
- 17 A. Moropoulou, A. Bakolas and K. Bisbikou, *Constr. Build. Mater.*, 14 (2000) 35.
- 18 A. Moropoulou, A. Bakolas and S. Anagnostopoulou, *Cem. Concr. Comp.*, 27 (2005) 295.
- 19 C. Genestar, C. Pons and A. Más, *Anal. Chim. Acta*, 557 (2006) 373.
- 20 M. J. Mosquera, D. Benitez and S. H. Perry, *Cem. Concr. Res.*, 32 (2002) 1883.
- 21 D. Benavente, M. A. Garcia del Cura, R. Fort and S. Ordóñez, *J. Cryst. Growth*, 204 (1999) 168.
- 22 G. W. Scherer, *Cem. Concr. Res.*, 29 (1999) 1347.

Received: December 28, 2006

Accepted: May 29, 2007

DOI: 10.1007/s10973-006-8313-8